



Article

Panchromatic Light-Absorbing [70]Fullerene-Perylene-BODIPY Triad with Cascade of Energy Transfer as an Efficient Singlet Oxygen Sensitizer

Lifeng Dou^{1,†}, Yuanming Li^{2,†}, Lei Dong¹, Shuao Zhang¹, Yuanqi Wu¹, Yu Gong¹, Wei Yang¹, Hongdian Lu¹, Sane Zhu^{1,3,*} and Xiaoguo Zhou^{2,*}

¹ School of Energy, Materials and Chemical Engineering, Hefei University, Hefei 230601, China; dou_lifeng2010@126.com (L.D.); 15955184794@139.com (L.D.); cloudrrrrrr@126.com (S.Z.); 13329282558@163.com (Y.W.); huayu202035@163.com (Y.G.); weyang@ustc.edu.cn (W.Y.); luhdo@hfu.edu.cn (H.L.)

² Hefei National Laboratory for Physical Sciences at the Microscale, Department of Chemical Physics, University of Science and Technology of China, Hefei 230026, China; liym@mail.ustc.edu.cn

³ State Key Laboratory of Fire Science, University of Science and Technology of China, Hefei 230026, China

* Correspondence: zhuse@hfu.edu.cn (S.Z.); xzhou@ustc.edu.cn (X.Z.); Tel.: +86-551-62158394 (S.Z.); +86-551-63600031 (X.Z.)

† These authors contributed equally to this work.

Abstract: A panchromatic light-absorbing [70]fullerene-peryene-BODIPY triad (**C₇₀-P-B**) was synthesized and applied as a heavy atom-free organic triplet photosensitizer for photooxidation. The photophysical processes were comprehensively investigated by the methods of steady-state spectroscopy, time-resolved spectroscopy, as well as theoretical calculations. **C₇₀-P-B** shows a strong absorption ability from 300–620 nm. Efficient cascading intramolecular singlet-singlet energy transfer in **C₇₀-P-B** was confirmed by the luminescence study. The backward triplet excited state energy transfer from C₇₀ moiety to perylene then occurs to populate ³perylene*. Thus, the triplet excited states of **C₇₀-P-B** are distributed on both C₇₀ and perylene moiety with lifetimes of 23 ± 1 μs and 175 ± 17 μs, respectively. **C₇₀-P-B** exhibits excellent photooxidation capacity, and its yield of singlet oxygen reaches 0.82. The photooxidation rate constant of **C₇₀-P-B** is 3.70 times that of **C₇₀-Boc** and 1.58 times that of MB, respectively. The results in this paper are useful for designing efficient heavy atom-free organic triplet photosensitizers for practical application in photovoltaics, photodynamic therapy, etc.

Keywords: [70]fullerene; perylene; BODIPY; cascade; ping-pong; energy transfer; singlet oxygen



Citation: Dou, L.; Li, Y.; Dong, L.; Zhang, S.; Wu, Y.; Gong, Y.; Yang, W.; Lu, H.; Zhu, S.; Zhou, X. Panchromatic Light-Absorbing [70]Fullerene-Perylene-BODIPY Triad with Cascade of Energy Transfer as an Efficient Singlet Oxygen Sensitizer. *Molecules* **2023**, *28*, 3534. <https://doi.org/10.3390/molecules28083534>

Received: 19 March 2023

Revised: 6 April 2023

Accepted: 14 April 2023

Published: 17 April 2023



Copyright: © 2023 by the authors. Licensee MDPI, Basel, Switzerland. This article is an open access article distributed under the terms and conditions of the Creative Commons Attribution (CC BY) license (<https://creativecommons.org/licenses/by/4.0/>).

1. Introduction

For the wide application of singlet oxygen in the areas of photodynamic therapy (PDT) [1–4], in vivo oxygen sensing [5], bioimaging [3] and photocatalysis [6,7], researchers have been exploring ways to produce high yields of singlet oxygen in recent years. Singlet oxygen could be generated by photosensitizers (PSs) upon light irradiation in the presence of molecular oxygen. To achieve high photosensitizing efficiency, PSs should exhibit these characteristics, e.g., broadband absorption in the visible or NIR region, high efficiency of intersystem crossing (ISC), long triplet excited state lifetimes, and high photostability [8–10]. However, designing PSs with all of the overall properties is a challenge.

The most commonly used strategy for designing triplet PSs is the introduction of heavy atoms [8,11–13]. Although heavy-atoms can enhance the ISC to generate triplet states, these PSs still suffer from the weak absorption in the visible range, toxicity, and short triplet excited state lifetimes. A number of other strategies have also been developed to design PSs without heavy atoms, for instance, a twisted π-conjugation system [14,15], radical enhanced intersystem crossing [16], and spin-orbit charge transfer [17,18]. However,

there are no clear rules regarding the relationship between the ISC and molecular structure in order to improve singlet oxygen generation efficiency. Moreover, most of the reported PSs are mono-chromophoric, resulting in their narrow absorption in the visible or NIR region. To overcome these shortcomings, connecting multi-chromophores with an electron spin convertor is a good strategy to construct heavy atom free PSs [8]. Benefiting from the high ISC efficiency, unique properties in biological systems and easy functionalization, fullerenes (mainly C₆₀) are frequently employed as efficient spin convertors [7,19–22]. Significantly greater photosensitization efficiency has been achieved in C₆₀-based triplet PSs. C₇₀, a higher molecular weight fullerene, also possesses high ISC efficiency (near 1.0) [23]. Compared with C₆₀, C₇₀ has a much more extended system, higher absorption in the visible region, better photodynamic activity, and higher TTA quantum yield [24–26]. As a consequence, it is highly promising to synthesize PSs with higher performance using C₇₀ as a spin convertor. Until now, only a few C₇₀-based triplet photosensitizers have been reported [9,27].

In this study, we devised and synthesized a panchromatic light-absorbing [70]fullerene-perylene-BODIPY triad (C₇₀-P-B) as an efficient singlet oxygen sensitizer using amidation reactions. Considering the strong absorptions in the visible range (at about 505 nm), and energetically high lying excited states, BODIPY was selected as the light harvesting antenna [28]. Perylene, which shows strong absorptions from 525 nm to 620 nm, is complementary in terms of the absorptions to BODIPY. Thus, BODIPY and perylene were selected as light harvesting antennas, and C₇₀ was chosen as a spin convertor to form a cascade of the energy transfer system. Moreover, the rigid molecular structure can increase ISC rates and quantum yields by suppressing the vibronic deactivation [29]. Thus, BODIPY, perylene and C₇₀ were connected through rigid phenyl and biphenyl linkers, respectively. The structure of C₇₀-P-B is shown in Figure 1. To determine the photophysical properties and photooxidation capacity of C₇₀-P-B, C₇₀-Boc, PDI [29], BOD [30,31] and P-B are also prepared as reference compounds. For good solubility, C₇₀-Boc is synthesized to replace C₇₀ as the reference monomer. More stable PDI is also synthesized as a reference monomer to replace perylene. The structures of all the reference compounds are also given in Figure 1. As expected, C₇₀-P-B can efficiently harvest broadband excitation light to generate triplet states. The photophysical processes of C₇₀-P-B were comprehensively investigated by steady-state UV-visible absorption and fluorescence spectroscopy, time-resolved fluorescence spectroscopy, nanosecond time-resolved transient absorption spectroscopy, as well as theoretical calculations. Thanks to the panchromatic light-absorbing and cascade of energy transfer, C₇₀-P-B can be used as an efficient photosensitizer to generate singlet oxygen with a high yield. Therefore, our results are very useful for the design and preparation of efficient singlet oxygen sensitizers.

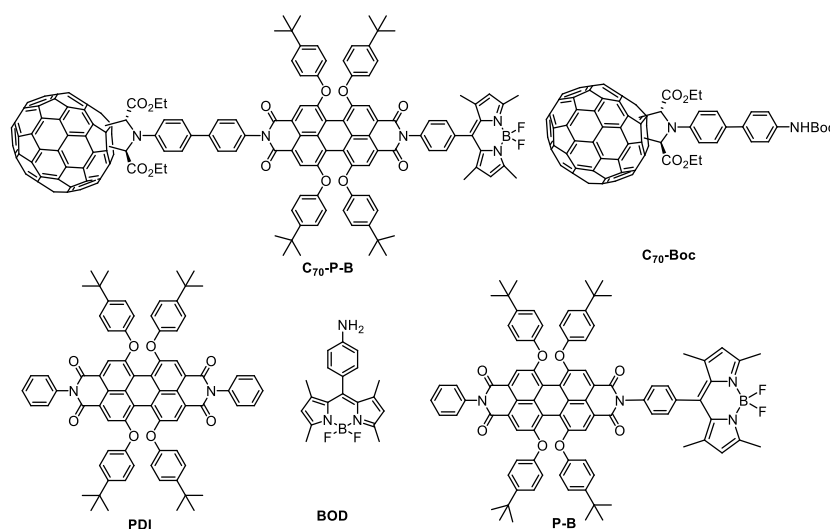
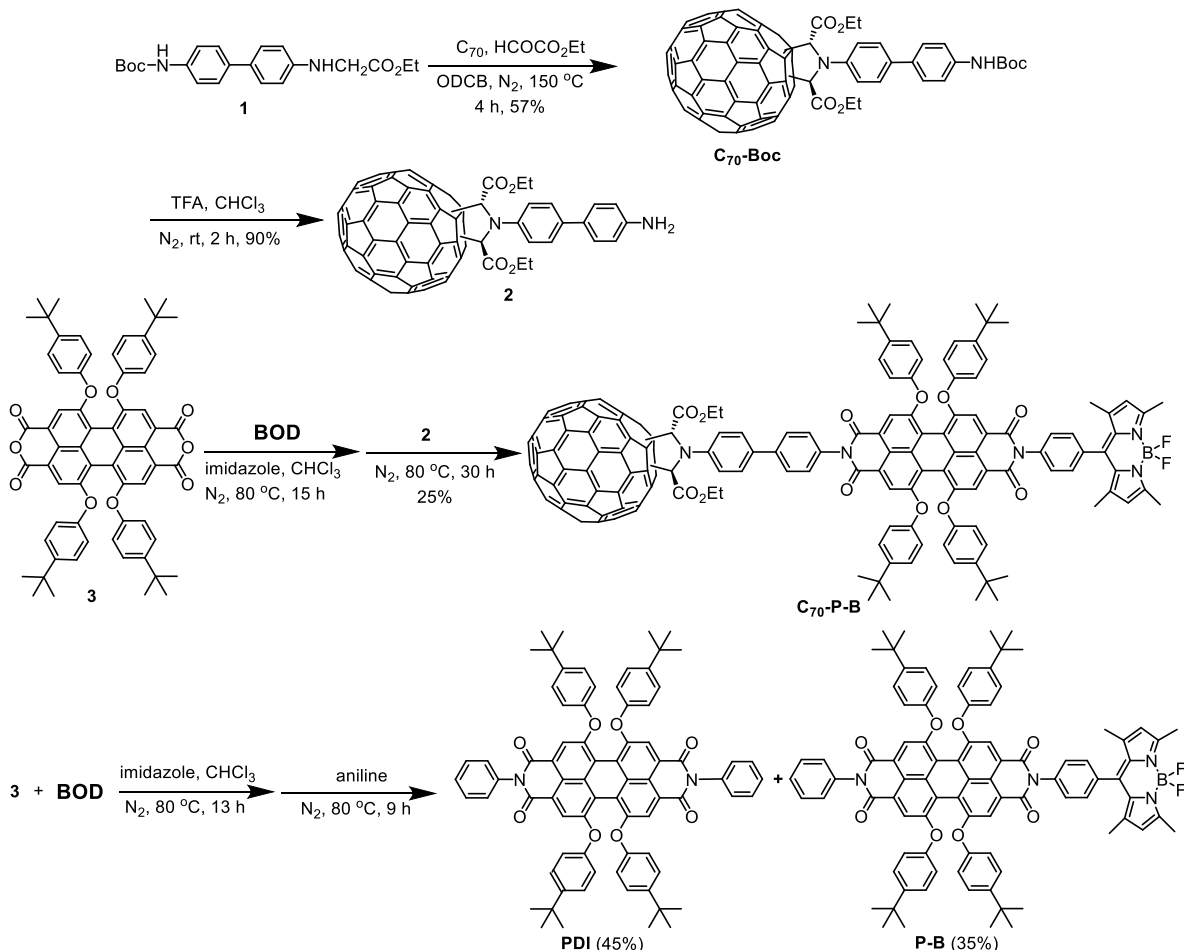


Figure 1. Molecules synthesized and studied in the present work.

2. Results

2.1. Synthesis

The synthetic routes of the triad **C₇₀-P-B** and the reference compounds are shown in Scheme 1, and the details are given in the Section 3.



Scheme 1. Synthetic procedures for **C₇₀-P-B**, the reference compounds **PDI** and **P-B**.

Compound **1** was synthesized according to the reported procedures of our group [30]. Next, **1** was reacted with glyoxylic acid ethyl ester and C₇₀ by 1,3-dipolar cycloaddition in *o*-dichlorobenzene (ODCB) at 150 °C for 4 h to provide **C₇₀-Boc** in 27% yield. Compound **2** could be prepared by removing the Boc-group with TFA. **BOD** was also synthesized following the procedures of our group [31,32]. **BOD** then was reacted with 3,4,9,10-perylenetetracarboxylic dianhydride (**3**) using imidazole as a base to afford the monoanhydride derivative. Monoanhydride has strong adsorption on a silica gel column, and thus it is difficult to get the pure product. Without characterization, the monoanhydride derivative was reacted directly with **2** to synthesize **C₇₀-P-B** in 25% yield.

Following the similar procedures, the reference compounds **PDI** and **P-B** were prepared by the cross-condensation of **3**, **BOD** and aniline in 41% and 31% yields, respectively.

The structures of all the new compounds were confirmed by NMR, MS and IR spectroscopy techniques. The NMR and MS spectra of all the compounds are given in the Supplementary Materials. For the sake of clarity, the expansions of the ¹H-NMR spectrum of **C₇₀-P-B** in CDCl₃ is shown in Figure 2.

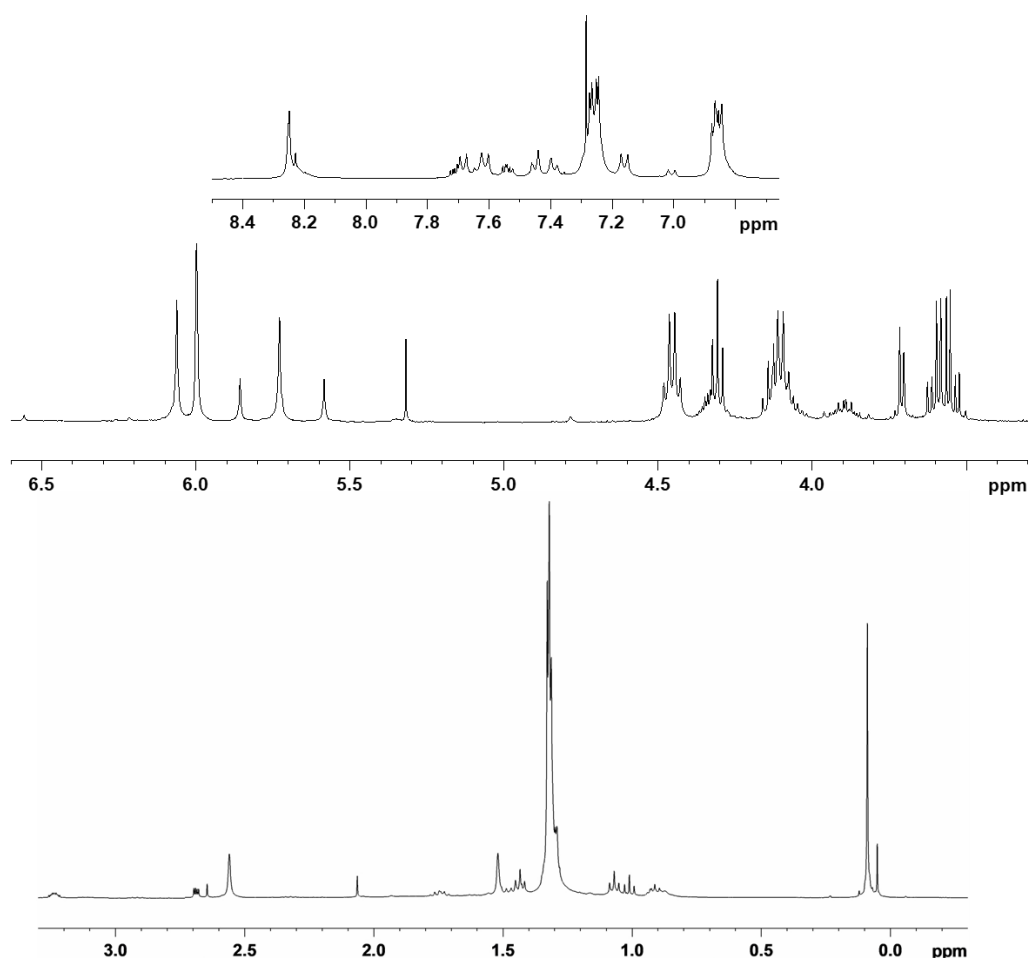


Figure 2. Expansions of ^1H NMR spectrum of $\text{C}_{70}\text{-P-B}$ in CDCl_3 .

The structural symmetry of C_{70} is D_{5h} , lower than that of C_{60} , and, therefore, C_{70} has four different [6,6] ring fusions with different reactivity [33]. As a result, $\text{C}_{70}\text{-P-B}$ and $\text{C}_{70}\text{-Boc}$ obtained by 1,3-dipolar cycloaddition are a mixture of isomers. From the ^1H NMR spectrum, it can be concluded that $\text{C}_{70}\text{-P-B}$ contains at least three isomers. The peaks at $\sim 8.25\text{--}8.19$ ppm are assigned to the perylene skeleton protons; peaks at $\sim 7.73\text{--}6.84$ ppm are assigned to phenyl ring protons; peaks at $\sim 6.01\text{--}5.32$ ppm are assigned to pyrrolidine protons and pyrrole ring protons; peaks at $\sim 4.48\text{--}3.52$ ppm are assigned to OCH_2CH_3 ; peaks at $\sim 2.64\text{--}2.06$ ppm are assigned to protons of pyrrole ring CH_3 , and peaks at $\sim 1.52\text{--}0.87$ ppm are assigned to OCH_2CH_3 , protons of the pyrrole ring CH_3 and $\text{C}(\text{CH}_3)_3$ of perylene. The ^{13}C NMR spectrum of $\text{C}_{70}\text{-P-B}$ also shows the expected signals. For example, the peaks from $169.53\text{--}163.01$ ppm are assigned to the carbons of $\text{C}=\text{O}$, the peaks from $157.42\text{--}118.97$ ppm are assigned to the $\text{sp}^2\text{-C}$ of C_{70} and the benzene ring, the peaks at $\sim 74.23\text{--}72.86$ ppm are carbons of CHCO_2 , the peaks from $70.88\text{--}70.38$ ppm are assigned the $\text{sp}^3\text{-C}$ of C_{70} , peaks from $65.40\text{--}60.33$ ppm are assigned the carbons of OCH_2CH_3 , peaks from $34.19\text{--}29.96$ ppm are carbons of $\text{C}(\text{CH}_3)_3$ and $\text{C}(\text{CH}_3)_3$, and peaks from $14.62\text{--}13.93$ ppm are carbons of CH_3 . The mass spectrum of $\text{C}_{70}\text{-P-B}$ gives a molecular peak at m/z 2482.7023, which is consistent with the calculated data.

2.2. UV-Vis Absorption and Steady-State Fluorescence

In order to investigate the photophysical properties of the $\text{C}_{70}\text{-P-B}$ triad and each component, the UV-vis absorption and steady-state fluorescence spectra of $\text{C}_{70}\text{-P-B}$ and the reference compounds were recorded and shown in Figure 3. $\text{C}_{70}\text{-Boc}$ with only one C_{70} moiety shows weak absorption in the visible range, and three absorption peaks are located at 398 nm ($\epsilon = 23,149 \text{ M}^{-1} \text{ cm}^{-1}$), 465 nm ($\epsilon = 17,772 \text{ M}^{-1} \text{ cm}^{-1}$) and 535 nm ($\epsilon = 9731 \text{ M}^{-1} \text{ cm}^{-1}$). P-B

with BODIPY and perylene moieties gives the characteristic absorption peaks of BODIPY at 503 nm and perylene at 575 nm. Intense absorptions at 306 nm ($\epsilon = 74,056 \text{ M}^{-1} \text{ cm}^{-1}$) corresponding to the absorption of C_{70} , 503 nm ($\epsilon = 67,654 \text{ M}^{-1} \text{ cm}^{-1}$) corresponding to the absorption of BODIPY, and 575 nm ($\epsilon = 49,166 \text{ M}^{-1} \text{ cm}^{-1}$) corresponding to the absorption of perylene are found for $\text{C}_{70}\text{-P-B}$. Compared with the monomers, the maximum absorption peaks of $\text{C}_{70}\text{-P-B}$ and P-B are redshifted by about 1 nm. The UV-vis spectrum of $\text{C}_{70}\text{-P-B}$ is nearly a superimposition of the monomers, suggesting that electronic communication between P-B and C_{70} is weak at the ground state.

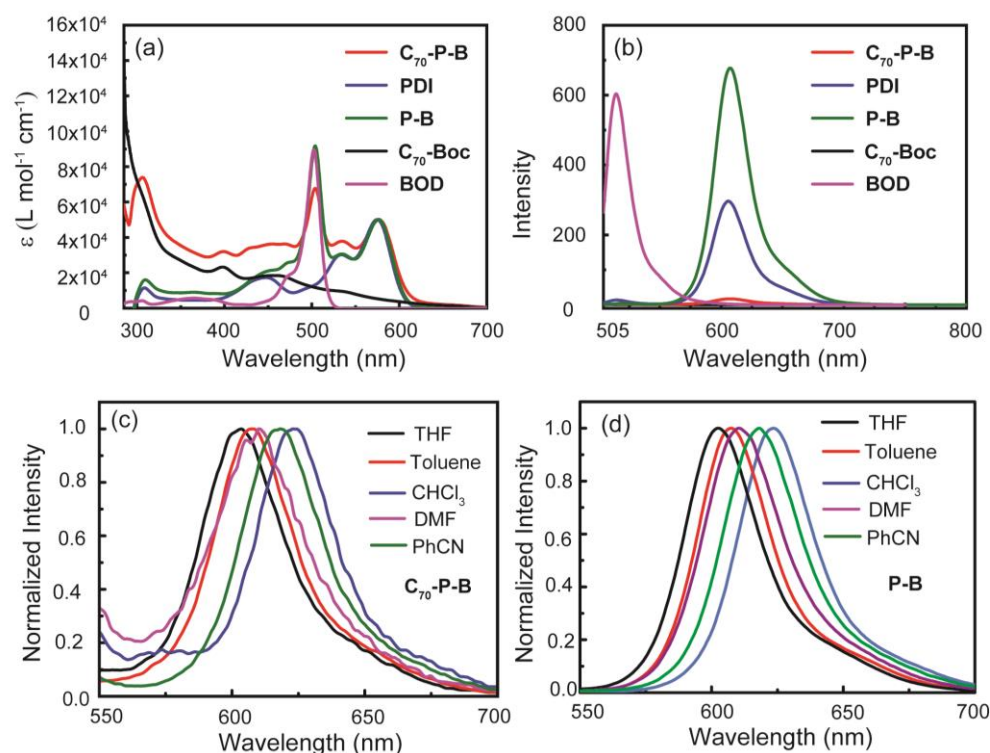


Figure 3. (a) UV-vis absorption and (b) fluorescence spectra of $\text{C}_{70}\text{-P-B}$, the reference compounds **PDI**, **P-B**, $\text{C}_{70}\text{-Boc}$ and **BOD** in toluene ($c = 1.0 \times 10^{-5} \text{ mol/L}$ for **PDI**, **P-B** and $\text{C}_{70}\text{-Boc}$, $c = 1.0 \times 10^{-6} \text{ mol/L}$ for **BOD**). Emission of (c) $\text{C}_{70}\text{-P-B}$ and (d) **P-B** in THF, CHCl_3 , DMF, PhCN and toluene. Exited at 489 nm.

The photoinduced intramolecular energy transfer of $\text{C}_{70}\text{-P-B}$ and **P-B** was confirmed by the luminescence study. The results are presented in Figure 3b. With photoexcitation at 489 nm, the emission peaks belonging to the C_{70} part in $\text{C}_{70}\text{-Boc}$ and $\text{C}_{70}\text{-P-B}$ were not detected due to the extremely low fluorescence quantum yield of C_{70} [34–36], as well as the overlapping by the fluorescence emission of perylene. In the same conditions, **BOD** gives an intense fluorescence at 514 nm, whereas, due to the efficient intramolecular energy transfer from BODIPY to perylene, this emission is almost completely quenched in both $\text{C}_{70}\text{-P-B}$ and **P-B**. $\text{C}_{70}\text{-P-B}$, **P-B** and **PDI** exhibit similar spectral characteristics with an emission peak at 607 nm corresponding to the perylene unit [37,38]. Compared with **PDI**, the luminescence intensity of **P-B** at 607 nm is largely enhanced (the luminescence intensity of **P-B** is 2.27 times that of **PDI**) due to the direct excitation of the perylene moiety and the energy transfer from the BODIPY moiety to perylene upon photoexcitation. Compared with the luminescence intensities of **PDI** and **P-B**, the emission corresponding to perylene moiety is largely quenched in $\text{C}_{70}\text{-P-B}$ by the introduction of C_{70} . The quenching efficiency of $\text{C}_{70}\text{-P-B}$ is about 97% compared to **P-B**. The emission quenching of perylene in $\text{C}_{70}\text{-P-B}$ should be ascribed to the efficient excitation energy transfer from perylene to C_{70} upon BODIPY part excitation. The intramolecular energy transfer from the perylene part to C_{70}

is thermodynamically allowed, because the energy of the S_1 state of perylene (2.16 eV) is higher than that of C_{70} (1.85 eV) [9].

To further investigate the effect of solvent polarity on luminescence, the fluorescence emissions of C_{70} -**P-B** and **P-B** in THF, $CHCl_3$, DMF, PhCN and toluene at the same concentration were measured, as shown in Figure 3c,d. The fluorescence emission intensities are normalized. Clear shifts in emission peaks of C_{70} -**P-B** and **P-B** in different solvents could be observed due to the change in dipole moments. Both emission peaks of C_{70} -**P-B** and **P-B** are solvent sensitive [30,39].

2.3. Time-Resolved Fluorescence Spectroscopy

To further study the photo induced intramolecular energy transfer process, the transient fluorescence emission of C_{70} -**P-B**, **P-B** and **PDI** were investigated, and a single exponential fit was applied mathematically to all of these compounds. The results are shown in Figure 4.

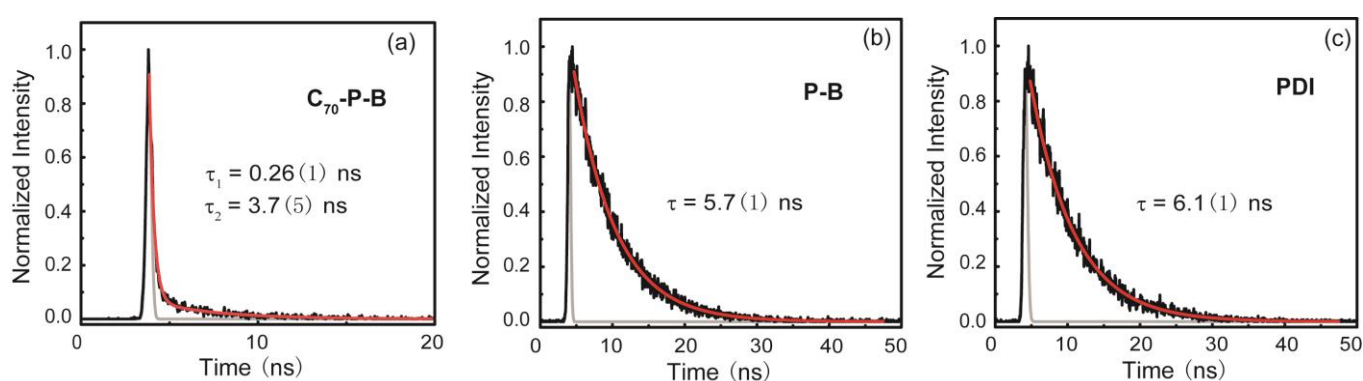


Figure 4. Fluorescence decay traces obtained with a time-correlated single photon counting (TCSPC) of (a) C_{70} -**P-B**, (b) **P-B** and (c) **PDI** in toluene. They were excited at 510 nm and recorded at 600 nm. The gray lines are the instrument response profiles, black lines are the raw data, and the red lines are the fitting curves. The brackets represent the error of fitting.

With photoexcitation at 510 nm, the fluorescence signal at 600 nm was obtained for all three compounds. As shown in Figure 4, all fluorescence decay curves can be perfectly fitted by a single exponential process, and a fast-decay component (gray line, visible in Figure 4a with the full width at half maximum of 0.26 ns), is attributed to the instrument response profile [40]. As a result, the fluorescence lifetimes are determined to be 3.7 ± 0.5 ns for C_{70} -**P-B**, 5.7 ± 0.1 ns for **P-B**, and 6.1 ± 0.1 ns for **PDI**, respectively. The lifetime of C_{70} -**P-B** is apparently shorter than that of **P-B** and **PDI**, and close to the intrinsic lifetime of the C_{70} monomer [36], providing extra evidence for the formation of ${}^1C_{70}^*P-B$ by intramolecular energy transfer. C_{70} -**P-B** undergoes significant attenuation relative to that of **P-B**, indicating that after the introduction of C_{70} , the excited state energy of perylene can be quenched via energy transfer. The results are consistent with that obtained in the steady-state fluorescence spectra.

2.4. Nanosecond Time-Resolved Transient Absorption Spectroscopy

To delve into the triplet state properties of C_{70} -**P-B** and C_{70} -**Boc**, nanosecond time-resolved transient absorption spectra were recorded with photoexcitation at 532 nm, and are displayed in Figure 5a,c, respectively.

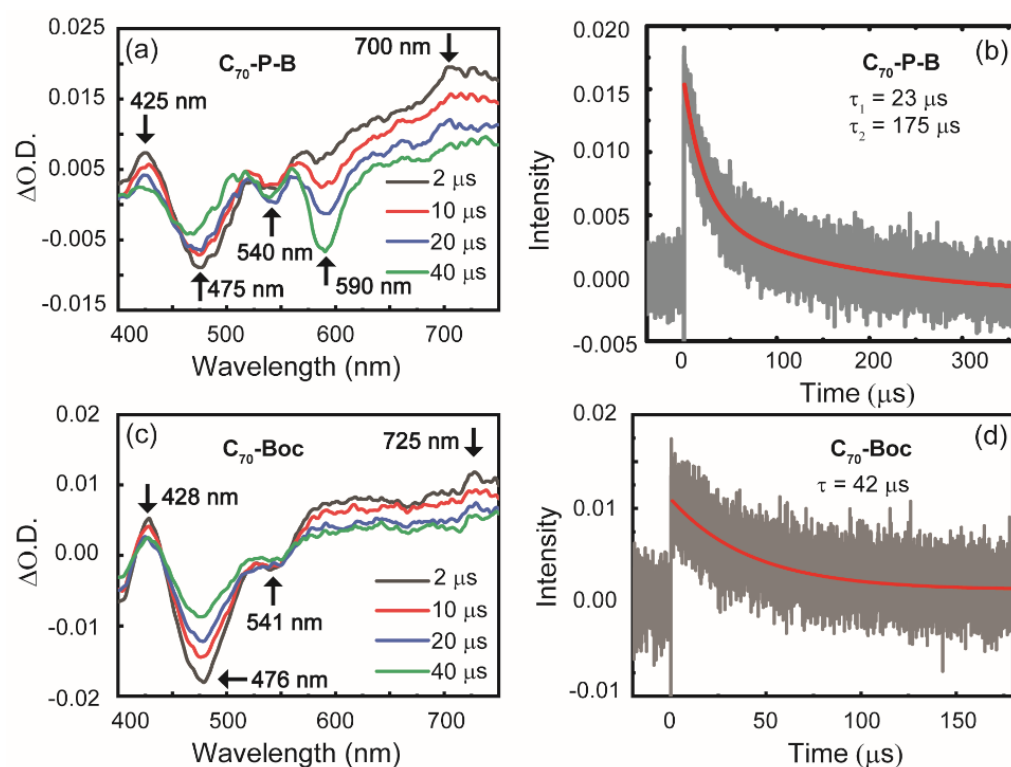


Figure 5. Nanosecond time-resolved transient absorption spectra of (a) C_{70} -P-B and (c) C_{70} -Boc upon excitation at 532 nm with a pulse laser (10 ns, 8 mJ/pulse) in deaerated toluene at room temperature. Decay curves of (b) C_{70} -P-B and (d) C_{70} -Boc at 700 nm. Arrows indicate the spectral trend with time increasing. The gray lines are the raw data, and the red lines are the fitting curves.

For C_{70} -Boc, a negative peak at 476 nm and two positive absorption bands at 428 nm and \sim 700 nm were observed. The negative peak could be attributed to the ground-state bleaching (GSB) peak due to its similar position to the absorption of C_{70} -Boc, while the two positive bands originate from the triplet absorption of the C_{70} moiety. For C_{70} -P-B, in addition to the three bands at 425 nm, 475 nm and \sim 700 nm, similar to C_{70} -Boc, a curiously negative peak at 590 nm was gradually generated. The global fit shows that this negative peak is generated with a characteristic time of $30 \pm 2 \mu$ s, and is attenuated with a lifetime of $176 \pm 11 \mu$ s (Figure S1). In comparison with the steady-state absorption spectrum, the negative peak is close to the absorption position of the perylene moiety, and can therefore be attributed to the GSB of the perylene. Considering that the GSB of C_{70} at 475 nm and of perylene at 590 nm shows completely distinct evolution dynamics, it is inferred that there are two different triplet states of this photosensitizer. This deduction could also be verified by the dynamic decay behaviors of C_{70} -P-B and C_{70} -Boc at 700 nm. By fitting the kinetic curve of C_{70} -Boc, the decay of the C_{70} triplet state was identified as mono-exponential, with a lifetime of $42 \pm 2 \mu$ s. However, the decay process of C_{70} -P-B was fitted to a bi-exponential form, possessing a short lifetime of $23 \pm 1 \mu$ s and a longer lifetime of $175 \pm 17 \mu$ s (Figure 5b). Coincidentally, these two lifetimes matched up with the generation and decay lifetimes of the GSB for perylene. Combined with the result of transient absorption spectra, the shorter lifetime should be ascribed to the triplet state of C_{70} ; the longer one is the triplet state of perylene. Thus, we propose that the backward triplet energy transfer from C_{70} to the perylene moiety occurs, which also explains why the lifetime of the triplet state of the C_{70} part in the triad is shorter than that in C_{70} -Boc.

Considering the results of steady-state fluorescence and time-resolved fluorescence spectroscopy parts, a “ping-pong” energy transfer mechanism is proposed for the decay dynamics of C_{70} -P-B upon photoexcitation. When the BODIPY part is excited, it can transfer energy to the perylene moiety to produce 1 perylene*. Singlet energy transfer from

$^1\text{perylene}^*$ to C_{70} and efficient ISC processes leads to the formation of $^3\text{C}_{70}^*$. According to the optimized geometry of $\text{C}_{70}\text{-P-B}$, as shown in Figure S2, the distance between the BODIPY and perylene units is around 15 Å, and that between the perylene and C_{70} moieties is more than 20 Å. Therefore, Förster energy transfer should dominate for the intramolecular singlet-singlet energy transfer. The backward triplet excited state energy transfer from $^3\text{C}_{70}^*$ to perylene then occurs to populate the $^3\text{perylene}^*$.

2.5. TD-DFT Calculations

To validate the energy transfer mechanism mentioned above, density functional theory (DFT) was adapted to calculate the optimized geometry, electronic configuration, vertical excitation energies, and frontier molecular orbitals of $\text{C}_{70}\text{-P-B}$. The optimized structure of $\text{C}_{70}\text{-P-B}$ is shown in Figure S2, and the computational details are also available in the Supplementary Materials section.

Figure 6 shows the transition features of the two lowest triplet states, which are attributed to the HOMO→LUMO+2 and HOMO-3→LUMO transitions, respectively. Moreover, HOMO and LUMO+2 are primarily distributed on the perylene group, whereas HOMO-3 and LUMO are mostly located on the C_{70} moiety. Consequently, these two transitions are the local excitation for perylene and C_{70} , respectively, hence the designations $\text{C}_{70}\text{-}^3\text{P}^*\text{-B}$ and $^3\text{C}_{70}^*\text{-P-B}$. Moreover, as shown in Figure 6, the excitation energies of $^3\text{C}_{70}^*\text{-P-B}$ and $\text{C}_{70}\text{-}^3\text{P}^*\text{-B}$ are calculated to be 1.48 and 1.14 eV, respectively. The slightly high energy of $^3\text{C}_{70}^*\text{-P-B}$ confirms that the triplet energy transfer from the C_{70} moiety to the perylene unit in the triad is thermodynamically feasible, which is in line with our experimental conclusions.

2.6. Photooxidation of 1,5-Dihydroxy Naphthalene Mediated by $^1\text{O}_2$

Using $\text{C}_{70}\text{-P-B}$, $\text{C}_{70}\text{-Boc}$ and P-B as singlet oxygen sensitizers, their photooxidation properties were explored by using DHN as a chemical sensor and MB as a reference.

In the presence of $^1\text{O}_2$, DHN can be easily oxidized to juglone. The photooxidation kinetics can be measured by following the decrease in the absorption of DHN at 301 nm or the increase in the absorption of juglone at 427 nm with time. The spectral responses of DHN using $\text{C}_{70}\text{-P-B}$, $\text{C}_{70}\text{-Boc}$, P-B and MB as the sensitizers upon excitation with a xenon lamp are presented in Figure 7 and Figure S3, respectively. For $\text{C}_{70}\text{-P-B}$, $\text{C}_{70}\text{-Boc}$ and MB, the change of the absorption at 301 nm is obvious, indicating the significant consumption of DHN and the efficient photosensitization ability of the triplet PSs, whereas, nearly no UV-vis absorption change is observed in the spectral responses of DHN with P-B as the photosensitizer. The photostability of $\text{C}_{70}\text{-P-B}$ was also investigated by exposing it to light for 1 h, and no decrease was observed in the absorption (Figure S4). This further proves that the decrease in the absorption at 301 nm is caused by photooxidation instead of the decomposition of the photosensitizers.

The photooxidation ability of the triplet photosensitizers was quantitatively compared by plotting the $\ln[(A - A')/A_0]$ against the irradiation time. The photooxidation rate constant and the yield of singlet oxygen (Φ_Δ), together with other photophysical properties of the photosensitizers, were calculated and are listed in Table 1.

Table 1. The photophysical properties of the photosensitizers.

Photosensitizers	λ_{abs}^a	λ_{F}^b	τ_{F}^c	τ_{T}^d	$k_{\text{obs}}^e/\text{min}^{-1}$	v_i^f	Φ_Δ^g
C₇₀-P-B	306, 399, 503, 575	607	3.7	175, 23	83.3	8.33	0.82
C₇₀-Boc	398, 465, 535	-	-	42	22.5	2.25	0.81 ^h
B-P	503, 575	607	5.7	-	3.7	0.37	-
MB	-	-	-	-	52.7	5.27	0.57

^a $c = 1.0 \times 10^{-5}$ M, in nm. ^b Fluorescence emission maximum, in nm. ^c Fluorescence lifetime, in ns. ^d Triplet state lifetime, in μs . ^e In DCM/MeOH (v/v) = 9/1. $c = 10^{-5}$ M. The rate constant k_{obs} was calculated by the formula: $\ln[(A - A')/A_0] = -k_{\text{obs}}t$. In 10^{-3} min^{-1} . ^f Initial consumption rate of DHN, $v_i = k_{\text{obs}}[\text{DHN}]$. In $10^{-6} \text{ M min}^{-1}$. ^g Quantum yield of singlet oxygen ($^1\text{O}_2$), with MB as standard ($\Phi_\Delta = 0.57$ in CH_2Cl_2). ^h Literature values [23].

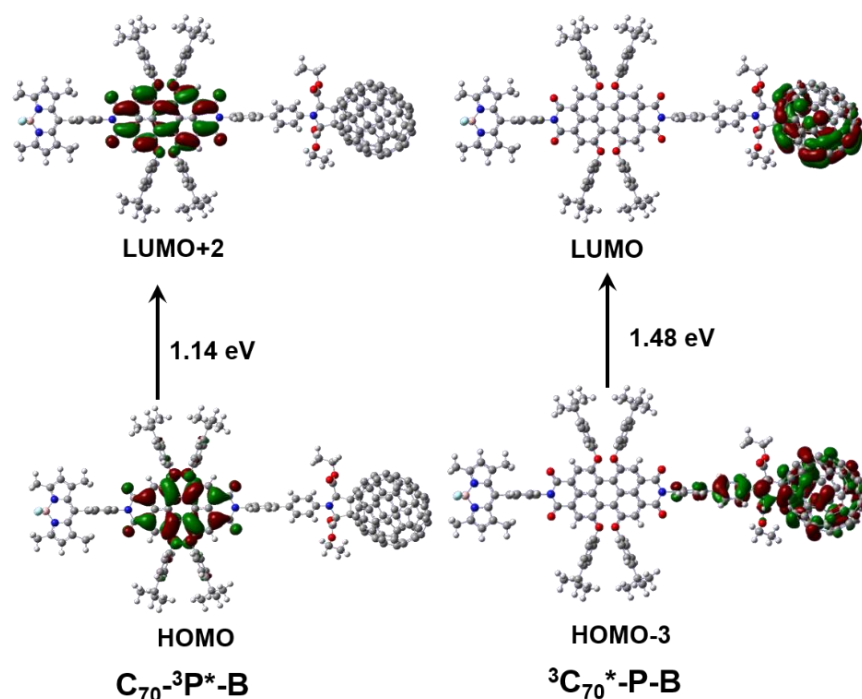


Figure 6. Frontier molecular orbitals involved in the triplet excited states of the C_{70} -P-B, in which the vertical excitation energy is labelled. The calculations were performed at the TD-DFT//B3LYP/6-31G(d) based on the DFT//B3LYP/6-31G(d) optimized ground state geometries using toluene as the solvent.

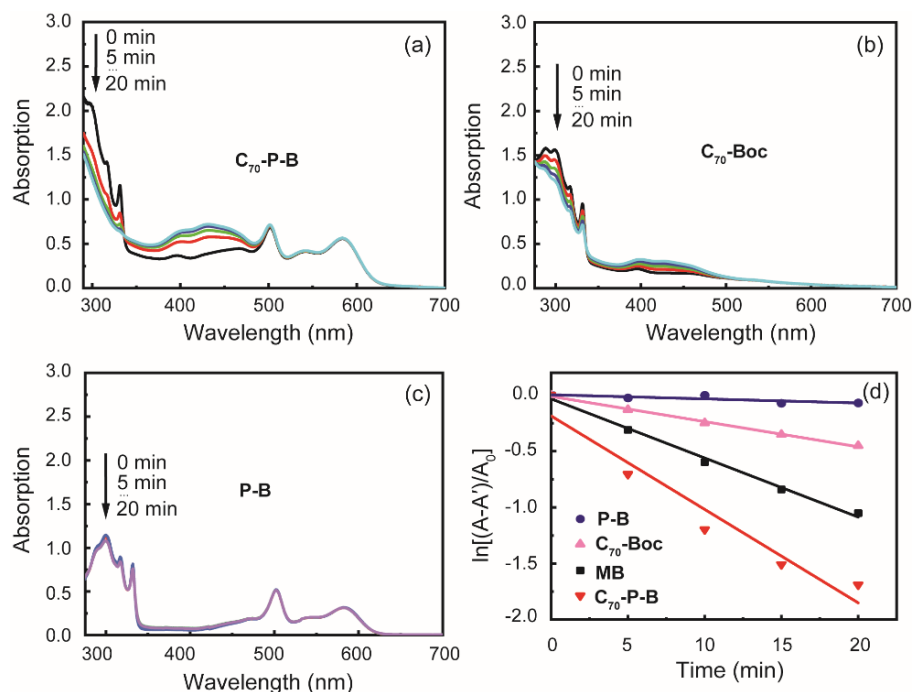


Figure 7. Absorption spectral evolution for the photooxidation of DHN using (a) C_{70} -P-B, (b) C_{70} -Boc and (c) P-B as photosensitizers. (d) Plots of $\ln[(A - A')/A_0]$ vs. irradiation time (t) for the photooxidation of DHN using different sensitizers (collected at 301 nm). $c[\text{sensitizers}] = 1.0 \times 10^{-5} \text{ mol L}^{-1}$, $c[\text{DHN}] = 1.0 \times 10^{-4} \text{ mol L}^{-1}$. In $\text{CH}_2\text{Cl}_2/\text{MeOH}$ (9:1, v/v). A and A_0 were the absorbances at 301 nm, where A was the absorption of DHN and sensitizer, A_0 was the absorption of sensitizer, and A' was the initial absorption of DHN.

3. Materials and Methods

3.1. Materials

All reagents were obtained from commercial sources. The C₇₀, 1,6,7,12-tetra-tert-butylphenoxyperylene-3,4,9,10-tetracarboxylic dianhydride, ethyl glyoxylate, chloroform-*d* (CDCl₃), trifluoroacetic acid (TFA), anhydrous sodium sulphate (Na₂SO₄) and DHN were purchased from Alfa Aesar. The imidazole, aniline, and 1,2-dichlorobenzene (ODCB) were purchased from J&K Scientific Ltd. (Beijing, China). The silica gel, carbon disulfide (CS₂), dichloromethane (DCM), petroleum ether (PE), methanol (MeOH), tetrahydrofuran (THF), trichloromethane (CHCl₃), and toluene were purchased from Sinopharm Chemical Reagent Co., Ltd. (Shanghai, China). THF was distilled over the sodium and benzophenone, while other reagents used for the synthesis were used directly.

All compounds were characterized by ¹H and ¹³C NMR spectroscopy on a BRUKER 400 MHz spectrometer. The mass analyses were performed using a Bruker ultrafleXtreme MALDI TOF/TOF (Bremen, Germany).

3.2. Synthesis

3.2.1. Synthesis of C₇₀-Boc

C₇₀ (200.0 mg, 0.24 mmol), compound **1** [30] (180.0 mg, 0.48 mmol) and ODCB (8 mL) were added into a 25 mL, three-neck flask equipped with a gas inlet adaptor. The mixture was stirred at room temperature under an N₂ atmosphere for 1 h. The ethyl glyoxylate solution (550 μL, 2.8 mmol) was added immediately, and the mixture was stirred at 150 °C for 4 h. The solvent was then removed, and the mixture was subjected to column chromatography on silica gel with CS₂/CH₂Cl₂ (3:2) as eluent to give C₇₀-Boc as a brown orange powder (83.9 mg, 27%). ¹H NMR (400 MHz, CDCl₃) δ 7.49 (d, *J* = 8.7 Hz, phenyl ring H), 7.45–7.43 (m, phenyl ring H), 7.41–7.34 (m, phenyl ring H), 7.07 (d, *J* = 8.7 Hz, phenyl ring H), 6.91 (d, *J* = 8.8 Hz, phenyl ring H), 6.41 (bs, NHBoc), 6.39 (bs, NHBoc), 6.00 (s, CHCO₂), 5.78 (s, CHCO₂), 5.67 (s, CHCO₂), 5.50 (s, CHCO₂), 4.40 (q, *J* = 7.1 Hz, OCH₂CH₃), 4.31–4.23 (m, OCH₂CH₃), 4.10–4.02 (m, OCH₂CH₃), 3.88–3.78 (m, OCH₂CH₃), 1.52 (s, OC(CH₃)₃), 1.51 (s, OC(CH₃)₃), 1.40 (t, *J* = 7.1 Hz, OCH₂CH₃), 1.29 (t, *J* = 7.1 Hz, OCH₂CH₃), 1.04 (t, *J* = 7.1 Hz, OCH₂CH₃), 0.87 (t, *J* = 7.1 Hz, OCH₂CH₃). ¹³C NMR (100 MHz, CS₂/CDCl₃ with Cr(acac)₃ as relaxation reagent) δ 170.05, 169.99, 169.47, 157.63, 155.31, 155.11, 154.62, 152.76, 151.53, 151.46, 151.23, 151.18, 150.92, 150.83, 150.80, 150.61, 150.50, 150.38, 150.00, 149.97, 149.85, 149.43, 149.32, 149.22, 149.18, 148.94, 148.83, 148.80, 147.56, 147.53, 147.29, 147.25, 147.16, 147.06, 147.01, 146.92, 146.31, 146.26, 146.20, 146.11, 146.05, 145.95, 144.55, 143.72, 143.58, 143.55, 143.51, 143.40, 143.28, 143.24, 141.09, 140.45, 140.41, 140.17, 138.20, 137.48, 137.44, 135.27, 135.23, 134.65, 133.89, 133.75, 133.17, 132.50, 132.25, 131.93, 131.72, 131.52, 131.49, 131.33, 127.71, 127.58, 127.29, 127.23, 119.05, 118.90, 118.85, 80.68, 74.48, 73.20, 72.86, 70.70, 64.82, 63.98, 62.30, 62.08, 61.90, 61.70, 61.68, 29.89, 28.48, 14.65, 14.52, 14.33, 14.13. FT-IR ν/cm⁻¹ (KBr) 2922, 2851, 1731, 1611, 1504, 1428, 1401, 1367, 1260, 1158, 1021, 818, 796, 534. HRMS (MALDI-TOF) *m/z* calcd for C₉₅H₃₀N₂O₆ [M⁻] 1294.2109, found 1294.2104.

3.2.2. Synthesis of Compound 2

C₇₀-Boc (100.0 mg, 0.08 mmol) was dissolved in chloroform (10 mL). The mixture was stirred under an N₂ atmosphere at room temperature for 10 min. TFA (2 mL) was then added, and the mixture was stirred at room temperature for 1.5 h until C₇₀-Boc disappeared. The mixture was purified on a silica gel column using CS₂/CH₂Cl₂ (1:4) as eluent to give compound **2** as a brown orange powder (87.7 mg, 95%). ¹H NMR (400 MHz, CDCl₃) δ 7.46 (d, *J* = 8.6 Hz, phenyl ring H), 7.35 (d, *J* = 8.7 Hz, phenyl ring H), 7.31 (d, *J* = 8.4 Hz, phenyl ring H), 7.25 (d, *J* = 8.5 Hz, phenyl ring H), 7.05 (d, *J* = 8.6 Hz, phenyl ring H), 6.89 (d, *J* = 8.6 Hz, phenyl ring H), 6.66 (d, *J* = 8.4 Hz, phenyl ring H), 6.62 (d, *J* = 8.5 Hz, phenyl ring H), 5.99 (s, CHCO₂), 5.78 (s, CHCO₂), 5.66 (s, CHCO₂), 5.50 (s, CHCO₂), 4.40 (q, *J* = 7.1 Hz, OCH₂CH₃), 4.30–4.22 (m, OCH₂CH₃), 4.05 (q, *J* = 8.0 Hz, OCH₂CH₃), 3.89–3.78 (m, OCH₂CH₃), 3.64 (bs, NH₂), 1.39 (t, *J* = 7.1 Hz, OCH₂CH₃), 1.28 (t, *J* = 7.1 Hz, OCH₂CH₃),

1.04 (t, $J = 7.1$ Hz, OCH_2CH_3), 0.96 (t, $J = 7.5$ Hz, OCH_2CH_3), 0.86 (t, $J = 7.1$ Hz, OCH_2CH_3). ^{13}C NMR (100 MHz, $\text{CS}_2/\text{CDCl}_3$ with $\text{Cr}(\text{acac})_3$ as relaxation reagent) δ 169.72, 169.69, 169.66, 157.53, 154.97, 154.53, 151.40, 151.32, 151.10, 151.05, 150.82, 150.67, 150.50, 150.38, 150.28, 149.87, 149.84, 149.73, 149.72, 149.30, 149.21, 149.09, 149.05, 148.80, 148.72, 147.44, 147.16, 147.11, 146.94, 146.81, 146.20, 146.16, 146.00, 145.95, 145.87, 145.52, 145.47, 143.47, 143.44, 143.41, 143.39, 143.17, 143.12, 142.88, 140.98, 140.34, 140.21, 140.06, 138.09, 137.33, 135.30, 133.76, 133.75, 133.63, 133.04, 131.20, 130.82, 127.64, 127.58, 127.18, 127.05, 119.06, 118.86, 115.43, 74.31, 73.32, 73.01, 72.74, 70.55, 64.71, 63.83, 62.06, 61.85, 61.67, 61.57, 61.45, 14.61, 14.48, 14.28, 14.09. FT-IR ν/cm^{-1} (KBr) 2963, 2922, 2834, 1731, 1622, 1501, 1428, 1400, 1262, 1180, 1095, 1022, 804, 534. HRMS (MALDI-TOF) m/z calcd for $\text{C}_{90}\text{H}_{22}\text{N}_2\text{O}_4$ [M^-] 1194.1585, found 1194.1589.

3.2.3. Synthesis of P-B

A mixture of **BOD** [31,32] (20.1 mg, 0.06 mmol), 1,6,7,12-tetra-tert-butylphenoxyperylene-3,4,9,10-tetracarboxylic dianhydride **3** (142.7 mg, 0.14 mmol), and imidazole (138.3 mg, 2.03 mmol) was stirred under an N_2 atmosphere at 80 °C in CHCl_3 (15 mL) for 13 h (monitored by TLC). Aniline (50 μL , 0.55 mmol) was then added, and the reaction mixture was allowed to react at 80 °C for 9 h. The mixture was cooled to room temperature and washed with water. The aqueous phase was extracted with CHCl_3 , and the combined organic phase was dried over anhydrous Na_2SO_4 . After the solvent was removed, the residue was purified by column chromatography on silica gel with toluene as the eluent to give **PDI** [30] (37.9 mg, 41%) and **B-P** (25.4 mg, 31%). **B-P**: ^1H NMR (300 MHz, CDCl_3) δ 8.29 (s, 2H), 8.24 (s, 2H), 7.53–7.38 (m, 7H), 7.23 (d, $J = 8.7$ Hz, 10H), 6.85 (dd, $J = 8.7$, 1.4 Hz, 8H), 6.00 (s, 2H), 2.55 (s, 6H), 1.50 (s, 6H), 1.28 (s, 18H), 1.26 (s, 18H); ^{13}C NMR (75 MHz, CDCl_3 with $\text{Cr}(\text{acac})_3$ as relaxation reagent) δ 163.67 (C=O), 163.64 (C=O), 156.47, 156.28, 155.94, 152.88, 152.87, 147.67, 143.37, 140.67, 136.16, 135.60, 135.29, 133.39, 133.27, 131.44, 129.82, 129.40, 129.14, 128.83, 128.63, 126.90, 126.84, 122.83, 122.39, 121.63, 121.16, 120.69, 120.23, 120.19, 119.93, 119.85, 119.59, 34.52, 31.56, 14.73, 14.65. FT-IR ν/cm^{-1} (KBr) 2962, 1709, 1675, 1589, 1545, 1506, 1406, 1340, 1317, 1284, 1198, 1085, 982, 879, 834, 751. MALDI-TOF-MS m/z calcd for $\text{C}_{89}\text{H}_{80}\text{BF}_2\text{N}_4\text{O}_8$ [M^-] 1380.5959, found 1380.6159.

3.2.4. Synthesis of C₇₀-P-B

Compound **3** (167.7 mg, 0.17 mmol), **BOD** [31,32] (25.8 mg, 0.07 mmol) and imidazole (108.5 mg, 1.61 mmol) were dissolved in 15 mL of chloroform and stirred for 30 min under an N_2 atmosphere. The flask was equipped with an airproof stopper and stirred at 80 °C for 15 h monitored by TLC. Upon completion of the reaction, the reaction mixture was carefully quenched by water (50 mL). The mixture was transferred to a 250 mL separatory funnel. The aqueous layer was extracted with dichloromethane (2×50 mL). The combined organic layer was washed with saturated brine (200 mL), dried with anhydrous sodium sulfate, filtered, and concentrated. The residue was purified by TLC using $\text{CH}_2\text{Cl}_2/\text{PE}$ (5:2) as an eluent to give monoanhydride as a crude product (43.6 mg, 50%). Without characterization, the crude monoanhydride was used directly. The crude monoanhydride, compound **2** (47.8 mg, 0.04 mmol), and imidazole (141.4 mg, 2.08 mmol) were dissolved in 6.5 mL of chloroform and stirred for 30 h under N_2 atmosphere at 80 °C. Upon completion of the reaction, the reaction mixture was carefully quenched by water (50 mL). The mixture was transferred to a 250 mL separatory funnel and extracted with dichloromethane (2×50 mL). The combined organic layer was washed with saturated brine (200 mL), dried with anhydrous sodium sulfate, filtered and concentrated. The residue was purified on a silica gel column using $\text{CH}_2\text{Cl}_2/\text{PE}/\text{CS}_2$ (5:1:1) as eluent to give **C₇₀-P-B** as a reddish brown solid (43.4 mg, 25%). ^1H NMR (400 MHz, CDCl_3) δ 8.25–8.198 (m, phenyl ring H), 7.73–7.52 (m, phenyl ring H), 7.46–7.38 (m, phenyl ring H), 7.26 (dd, $J = 8.8$, 3.0 Hz, phenyl ring H), 7.16 (d, $J = 8.6$ Hz, phenyl ring H), 7.01 (d, $J = 8.7$ Hz, phenyl ring H), 6.86 (dd, $J = 8.6$, 4.3 Hz, phenyl ring H), 6.06–5.32 (s, protons of CHCO_2 and pyrrole ring), 4.48–4.43 (m, OCH_2CH_3), 4.36–4.29 (m, OCH_2CH_3), 4.16–4.02 (m, OCH_2CH_3), 3.96–3.85

(m, OCH₂CH₃), 3.37–3.52 (m, OCH₂CH₃), 2.64 (s, pyrrole ring CH₃), 2.56 (s, pyrrole ring CH₃), 2.06 (s, pyrrole ring CH₃), 1.52 (s, pyrrole ring CH₃), 1.43 (t, *J* = 7.0 Hz, OCH₂CH₃), 1.329 (s, C(CH₃)₃), 1.321 (s, C(CH₃)₃), 1.313 (s, C(CH₃)₃), 1.07 (t, *J* = 7.1 Hz, OCH₂CH₃), 1.01 (t, *J* = 7.4 Hz, OCH₂CH₃), 0.94–0.88 (m, OCH₂CH₃); ¹³C NMR (100 MHz, CS₂/CDCl₃ with Cr(acac)₃ as relaxation reagent) δ 169.53, 169.44, 168.97, 163.15, 163.01, 157.42, 156.18, 156.08, 155.81, 155.66, 155.08, 154.87, 154.40, 152.77, 152.70, 151.33, 151.25, 151.01, 150.92, 150.74, 150.60, 150.39, 150.30, 150.18, 149.80, 149.75, 149.65, 149.61, 149.23, 149.10, 149.02, 148.98, 148.69, 148.64, 148.61, 147.36, 147.34, 147.30, 147.29, 147.09, 147.02, 146.97, 146.86, 146.72, 146.07, 146.04, 145.93, 145.82, 145.75, 144.15, 143.42, 143.39, 143.33, 143.21, 143.12, 143.07, 140.85, 140.33, 140.22, 140.18, 139.98, 137.98, 135.88, 135.34, 133.87, 133.63, 133.54, 133.23, 133.12, 132.94, 132.34, 132.31, 132.05, 131.67, 131.51, 131.29, 131.26, 131.13, 130.73, 129.68, 128.90, 128.83, 128.78, 128.13, 128.01, 127.45, 126.73, 126.69, 122.83, 122.32, 121.52, 120.97, 120.61, 120.12, 119.73, 119.43, 119.39, 118.97, 74.23, 74.19, 72.87, 70.88, 70.47, 70.39, 65.40, 64.64, 63.77, 62.10, 61.90, 61.69, 61.51, 60.94, 60.33, 34.20, 31.42, 30.74, 29.96, 14.62, 14.60, 14.46, 14.27, 14.07, 13.93. FT-IR ν/cm⁻¹ (KBr) 2959, 2924, 2852, 1708, 1673, 1592, 1504, 1402, 1339, 1283, 1174, 1090, 796, 546. HRMS (MALDI-TOF) *m/z* calcd for C₁₇₃H₉₄BF₂N₅O₁₂ [M⁻] 2482.7001, found 2482.7023.

3.3. Photooxidation Experiment

The solutions of sensitizers **C₇₀-P-B**, **C₇₀-Boc**, **P-B**, MB in a concentration of 2.0 × 10⁻⁵ mol L⁻¹ and DHN in a concentration of 2.0 × 10⁻⁴ mol L⁻¹ in CH₂Cl₂/MeOH (9:1, *v/v*) were mixed in a volume ratio of 1:1. O₂ was then bubbled through the mixtures for 10 min, and a xenon lamp (0.17 mW/cm², using 0.72 M NaNO₂ aqueous solution as a cutoff filter) was used as a broadband light source to irradiate the mixtures. The spectral responses of the mixtures were monitored by a UV-vis spectrophotometer at intervals of 5 min.

The singlet oxygen quantum yield (Φ_Δ) was calculated by using Equation (1)

$$\Phi_{\Delta}(x) = \Phi_{\Delta}(\text{std}) \frac{k_{\text{obs}}(x) \cdot I(\text{std})}{k_{\text{obs}}(\text{std}) \cdot I(x)} \quad (1)$$

In this equation, Φ_Δ(*x*) and Φ_Δ(std) are the singlet oxygen generation quantum yield of the photosensitizers and MB. *k*_{obs}(*x*) and *k*_{obs}(std) were the absolute value of the slopes of ln[(*A* - *A'*)/*A*₀] versus the irradiation time for the photooxidation of DHN by photosensitizers and MB, respectively. *I*(*x*) and *I*(std) were the total light intensities absorbed by photosensitizers and MB, respectively.

3.4. Photostability Experiment

The photostability of **C₇₀-P-B** was measured in CH₂Cl₂/MeOH (9:1, *v/v*, 1.0 × 10⁻⁵ mol L⁻¹) and irradiated continuously for 1 h using a xenon lamp (0.20 mW/cm²). A UV-vis spectrophotometer was then used to record the spectral responses of **C₇₀-P-B** at 0 h and 1 h, respectively.

3.5. Measurement of Photophysical Properties

UV-Vis absorption and steady-state fluorescence were measured using an absorption spectrometer (UV-1800, Mapada, Shanghai, China) and a fluorescence spectrophotometer (FP8500, JASCO, Tokyo, Japan) at room-temperature. The fluorescence lifetimes of all the compounds were recorded via a time-correlated single photon counting (TCSPC) apparatus at room temperature, and a pulsed laser at 510 nm was used as the excitation source. The nanosecond transient absorption spectra were recorded with a home-built laser flash photolysis system. The pulsed excitation light was from the second harmonic 532 nm of a Q-Switched Nd:YAG laser (Dawa-100, Beamtech, Beijing, China) with a pulse duration of 8 ns and a 10-Hz repetition rate, and was intersected by a white light from a 500W Xenon lamp in a 10 mm × 10 mm quartz cuvette. In experiments, the pulse laser energy was set as ca.10 mJ/pulse to achieve a better signal-to-noise ratio. A monochromator equipped with a photomultiplier was used to record the transient absorption

spectra within the wavelength range of 400–750 nm, with a spectral resolution of less than 1 nm. A kinetic curve of intermediate length was averaged by multi-shots and recorded with an oscilloscope (TDS3052B, Tektronix, Beaverton, OR, USA). All of the solutions were deoxygenated by purging with high purity argon (99.99%) for about 20 min prior to the measurements.

4. Conclusions

In conclusion, a panchromatic light-absorbing **C₇₀-P-B** triad with a cascade of energy transfer has been synthesized. The photophysical processes of the triad were investigated using steady-state UV-visible absorption and fluorescence spectroscopy, time-resolved fluorescence spectroscopy, nanosecond time-resolved transient absorption spectroscopy, and theoretical calculations. After the efficient cascade of singlet excited energy transfer from BODIPY to perylene and then to **C₇₀** and the ISC process, the backward triplet excited state energy transfer from **C₇₀** to perylene moiety occurred to populate the ³perylene*. The nanosecond time-resolved transient absorption results show that the triplet excited states of **C₇₀-P-B** are distributed on both **C₇₀** and the perylene moiety. The bi-exponential decay processes are found in **C₇₀-P-B**. The shorter lifetime of the triplet state is 23 μs, and the longer one is 175 μs. For the synergistic effect of the antennas and **C₇₀**, **C₇₀-P-B** exhibits excellent photooxidation capacity. The photooxidation rate constant of **C₇₀-P-B** is 3.70 times as that of **C₇₀-Boc** and 1.58 times as that of MB, respectively. The yield of singlet oxygen of **C₇₀-P-B** is as high as 0.82. The results indicate that **C₇₀**-antennas that are panchromatic light-absorbing and have a cascade of energy transfer are useful structure motifs for generating high yields of singlet oxygen.

Supplementary Materials: The following supporting information can be downloaded at: <https://www.mdpi.com/article/10.3390/molecules28083534/s1>, The nanosecond time-resolved transient absorption decay curve of **C₇₀-P-B** at 590 nm (Supplementary Figure S1), computational details (Supplementary Figure S2), the spectral response of DHN with MB as the sensitizer (Supplementary Figure S3), the photostability of **C₇₀-P-B** (Supplementary Figure S4), ¹H NMR, ¹³C NMR spectra, and the high resolution mass spectra (Supplementary Figures S5–S16) are also provided.

Author Contributions: L.D. (Lifeng Dou) and Y.L. performed the experiments; Y.G., L.D. (Lei Dong), S.Z. (Shuao Zhang), Y.W., W.Y. and H.L. analyzed the data; X.Z. and S.Z. (Sane Zhu) conceived and designed the experiments; L.D. (Lifeng Dou), Y.L., X.Z. and S.Z. (Sane Zhu) wrote the paper. All authors have read and agreed to the published version of the manuscript.

Funding: This work was sponsored by the Project Commissioned by Hangzhou Yitian Technology Co., Ltd. entitled *Research on the Catalytic System for Crosslinking, Hydrolysis and Condensation of Silane*, the Project Commissioned by Hefei Anhe Lubrication Technology Co., Ltd. entitled *Research on the Development and Application of Photosensitive Fungicide*, the Project Commissioned by Anhui Qingke Ruijie New Material Co., Ltd. entitled *Design and Synthesis of Porphyrinyl Functional Colorants*, the Natural Science Foundation for Colleges and Universities in Anhui Province (No. 2022AH040251), the Anhui Provincial Excellent Scientific Research and Innovation Team (No. 2022AH010096), and the Graduate Innovation and Entrepreneurship Program (No. 21YCX48).

Institutional Review Board Statement: Not applicable.

Informed Consent Statement: Not applicable.

Data Availability Statement: The data presented in this study are available in the Supplementary Materials.

Conflicts of Interest: The authors declare that they have no conflict of interest.

Sample Availability: Samples of the compounds **C₇₀-P-B**, **P-B**, and **C₇₀-Boc** are available from the authors.

References

1. Yaraki, M.T.; Liu, B.; Tan, Y.N. Emerging strategies in enhancing singlet oxygen generation of nano-photosensitizers toward advanced phototherapy. *Nanomicro Lett.* **2022**, *14*, 123.
2. Cao, W.-W.; Zhu, Y.; Wu, F.-P.; Tian, Y.; Chen, Z.-M.; Xu, W.-J.; Liu, S.-Y.; Liu, T.-T.; Xiong, H. Three birds with one stone: Acceptor engineering of hemicyanine dye with NIR-II emission for synergistic photodynamic and photothermal anticancer therapy. *Small* **2022**, *18*, 2204851. [[CrossRef](#)] [[PubMed](#)]
3. Nguyen, V.N.; Yim, Y.; Kim, S.; Ryu, B.; Swamy, K.M.K.; Kim, G.; Kwon, N.; Kim, C.Y.; Park, S.; Yoon, J. Molecular design of highly efficient heavy-atom-free triplet BODIPY derivatives for photodynamic therapy and bioimaging. *Angew. Chem. Int. Ed.* **2020**, *59*, 8957–8962. [[CrossRef](#)]
4. Yokoi, K.; Yasuda, Y.; Kanbe, A.; Imura, T.; Aoki, S. Development of wireless power-transmission-based photodynamic therapy for the induction of cell death in cancer cells by cyclometalated iridium (III) complexes. *Molecules* **2023**, *28*, 1433. [[CrossRef](#)] [[PubMed](#)]
5. Spencer, J.A.; Ferraro, F.; Roussakis, E.; Klein, A.; Wu, J.; Runnels, J.M.; Zaher, W.; Mortensen, L.J.; Alt, C.; Turcotte, R.; et al. Direct measurement of local oxygen concentration in the bone marrow of live animals. *Nature* **2014**, *508*, 269–273. [[CrossRef](#)]
6. Ghogare, A.A.; Greer, A. Using singlet oxygen to synthesize natural products and drugs. *Chem. Rev.* **2016**, *116*, 9994–10034. [[CrossRef](#)] [[PubMed](#)]
7. Huang, L.; Cui, X.-N.; Therrien, B.; Zhao, J.-Z. Energy-funneling-based broadband visible-light-absorbing bodipy-C₆₀ triads and tetrads as dual functional heavy-atom-free organic triplet photosensitizers for photocatalytic organic reactions. *Chem. Eur. J.* **2013**, *19*, 17472–17482. [[CrossRef](#)]
8. Zhao, J.-Z.; Wu, W.-H.; Sun, J.-F.; Guo, S. Triplet photosensitizers: From molecular design to applications. *Chem. Soc. Rev.* **2013**, *42*, 5323–5351. [[CrossRef](#)]
9. Zhu, S.-E.; Zhang, J.-H.; Gong, Y.; Dou, L.-F.; Mao, L.-H.; Lu, H.-D.; Wei, C.-X.; Chen, H.; Wang, X.-F.; Yang, W. Broadband visible light-absorbing [70]fullerene-BODIPY-triphenylamine triad: Synthesis and application as heavy atom-free organic triplet photosensitizer for photooxidation. *Molecules* **2021**, *26*, 1243. [[CrossRef](#)]
10. Namkoong, G.; Mamun, A.A.; Ava, T.T. Impact of PCBM/C₆₀ electron transfer layer on charge transports on ordered and disordered perovskite phases and hysteresis-free perovskite solar cells. *Org. Electron.* **2018**, *56*, 163–169. [[CrossRef](#)]
11. Qin, Y.; Yuan, X.-M.; Wang, Y.; Che, Y.-Y.; Sun, L.; Zhao, J.-Z.; Xu, H.-J. Truxene-linked coumarin-corrole triad: Synthesis, photophysical properties and application in triplet-triplet annihilation upconversion. *Dye. Pigment.* **2022**, *208*, 110865. [[CrossRef](#)]
12. Yu, X.-K.; Gao, F.-R.; Zhao, W.-Y.; Lai, H.-X.; Wei, L.-L.; Yang, C.; Wu, W.-H. BODIPY-conjugated bis-terpyridine Ru (II) complexes showing ultra-long luminescence lifetimes and applications to triplet-triplet annihilation upconversion. *Dalton Trans.* **2022**, *51*, 9314–9322. [[CrossRef](#)] [[PubMed](#)]
13. Sasaki, Y.; Yanai, N.; Kimizuka, N. Osmium complex-chromophore conjugates with both singlet-to-triplet absorption and long triplet lifetime through tuning of the heavy-atom effect. *Inorg. Chem.* **2022**, *61*, 5982–5990. [[CrossRef](#)] [[PubMed](#)]
14. Hu, W.-B.; Liu, M.-Y.; Zhang, X.-F.; Shi, M.; Jia, M.-X.; Hu, X.-F.; Liu, L.-L.; Wang, T. Minimizing the electron donor size of donor-acceptor-type photosensitizer: Twisted intramolecular charge-transfer-induced triplet state and singlet oxygen formation. *J. Phys. Chem.* **2020**, *124*, 23558–23566. [[CrossRef](#)]
15. Dong, Y.; Dick, B.; Zhao, J.-Z. Twisted Bodipy derivative as a heavy-atom-free triplet photosensitizer showing strong absorption of yellow light, intersystem crossing, and a high-energy long-lived triplet state. *Org. Lett.* **2020**, *22*, 5535–5539. [[CrossRef](#)] [[PubMed](#)]
16. Wang, Z.-J.; Zhao, J.-Z.; Barbon, A.; Toffoletti, A.; Liu, Y.; An, Y.-L.; Xu, L.; Karatay, A.; Yaglioglu, H.G.; Yildiz, E.A.; et al. Radical-enhanced intersystem crossing in new Bodipy derivatives and application for efficient triplet-triplet annihilation upconversion. *J. Am. Chem. Soc.* **2017**, *139*, 7831–7842. [[CrossRef](#)] [[PubMed](#)]
17. Miao, J.-F.; Huo, Y.-Y.; Yao, G.-X.; Feng, Y.; Weng, J.-J.; Zhao, W.; Guo, W. Heavy atom-free, mitochondria-targeted, and activatable photosensitizers for photodynamic therapy with real-time in-situ therapeutic monitoring. *Angew. Chem. Int. Ed.* **2022**, *61*, e202201815. [[CrossRef](#)]
18. Lv, M.; Lu, X.-C.; Jiang, Y.-R.; Sandoval-Salinas, M.E.; Casanova, D.; Sun, H.-T.; Sun, Z.-R.; Xu, J.-H.; Yang, Y.-J.; Chen, J.-Q. Near-unity triplet generation promoted via spiro-conjugation. *Angew. Chem. Int. Ed.* **2022**, *61*, e202113190. [[CrossRef](#)]
19. Joseph, J.; Baurath, S.; Charisiadis, A.; Charalambidis, G.; Coutsolelos, A.G.; Guldi, D.M. Cascades of energy and electron transfer in a panchromatic absorber. *Nanoscale* **2022**, *14*, 9304–9312. [[CrossRef](#)]
20. Che, Y.-Y.; Yuan, X.-M.; Sun, L.; Xu, H.-J.; Zhao, X.-Y.; Cai, F.-J.; Liu, L.; Zhao, J.-Z. Truxene-bridged Bodipy fullerene tetrads without precious metals: Study of the energy transfer and application in triplet-triplet annihilation upconversion. *J. Mater. Chem. C* **2020**, *8*, 15839–15851. [[CrossRef](#)]
21. Siposova, K.; Petrenko, V.I.; Ivankov, O.I.; Musatov, A.; Bulavin, L.A.; Avdeev, M.V.; Kyzyma, O.A. Fullerenes as an Effective Amyloid Fibrils Disaggregating Nanomaterial. *ACS Appl. Mater. Inter.* **2020**, *12*, 32410–32419. [[CrossRef](#)]
22. Rašović, I. Water-soluble fullerenes for medical applications. *Mater. Sci. Technol.* **2016**, *33*, 777–794. [[CrossRef](#)]
23. Arbogast, J.W.; Foote, C.S. Photophysical Properties of C₇₀. *J. Am. Chem. Soc.* **1991**, *113*, 8886–8889. [[CrossRef](#)]
24. Liu, Q.-L.; Guan, M.-R.; Xu, L.; Shu, C.-Y.; Jin, C.; Zheng, J.-P.; Fang, X.-H.; Yang, Y.-J.; Wang, C.-R. Structural effect and mechanism of C₇₀-carboxyfullerenes as efficient sensitizers against cancer cells. *Small* **2012**, *8*, 2070–2077. [[CrossRef](#)]

25. Doi, Y.; Ikeda, A.; Akiyama, M.; Nagano, M.; Shigematsu, T.; Ogawa, T.; Takeya, T.; Nagasaki, T. Intracellular uptake and photodynamic activity of water-soluble [60]- and [70]fullerenes incorporated in liposomes. *Chem. Eur. J.* **2008**, *14*, 8892–8897. [[CrossRef](#)] [[PubMed](#)]
26. Moor, K.; Kim, J.H.; Snow, S.; Kim, J.H. [70]Fullerene-sensitized triplet-triplet annihilation upconversion. *Chem. Commun.* **2013**, *49*, 10829–10831. [[CrossRef](#)] [[PubMed](#)]
27. Wei, Y.-X.; Zheng, M.; Zhou, Q.-H.; Zhou, X.-G.; Liu, S.-L. Application of a bodipy-C₇₀ dyad in triplet-triplet annihilation upconversion of perylene as a metal-free photosensitizer. *Org. Biomol. Chem.* **2018**, *16*, 5598–5608. [[CrossRef](#)]
28. Zhang, X.-F. BODIPY photosensitizers based on PET and heavy atom effect: A comparative study on the efficient formation of excited triplet state and singlet oxygen in BODIPY dimers and monomers. *J. Photochem. Photobiol. A Chem.* **2018**, *355*, 431–443. [[CrossRef](#)]
29. Nagarajan, K.; Mallia, A.R.; Muraleedharan, K.; Hariharan, M. Enhanced intersystem crossing in core-twisted aromatics. *Chem. Sci.* **2017**, *8*, 1776–1782. [[CrossRef](#)] [[PubMed](#)]
30. Zhu, S.-E.; Liu, K.-Q.; Wang, X.-F.; Xia, A.-D.; Wang, G.-W. Synthesis and properties of axially symmetrical rigid visible light-harvesting systems containing [60]fullerene and perylenebisimide. *J. Org. Chem.* **2016**, *81*, 12223–12231. [[CrossRef](#)]
31. Zhu, S.-E.; Zhang, J.-H.; Dou, L.-F.; Li, N.; Hu, K.-H.; Gao, T.-Y.; Lu, H.-D.; Si, J.-Y.; Wang, X.-F.; Yang, W. Rigid axially symmetrical C₆₀-BODIPY triplet photosensitizers: Effect of bridge length on singlet oxygen generation. *New J. Chem.* **2020**, *44*, 20419–20427. [[CrossRef](#)]
32. Zhu, S.-E.; Wang, F.-D.; Liu, J.-J.; Wang, L.-L.; Wang, C.; Yuen, A.C.Y.; Chen, T.B.Y.; Kabir, I.I.; Yeoh, G.H.; Lu, H.-D.; et al. BODIPY coated on MXene nanosheets for improving mechanical and fire safety properties of ABS resin. *Compos. B Eng.* **2021**, *223*, 109130–109142. [[CrossRef](#)]
33. Yin, J.-J.; Jin, L.-M.; Liu, R.-L.; Li, Q.-N.; Fan, C.-H.; Li, Y.; Li, W.-X.; Chen, Q.-Y. Reactions of fullerenes with reactive methylene organophosphorus reagents: Efficient synthesis of organophosphorus group substituted C₆₀ and C₇₀ derivatives. *J. Org. Chem.* **2006**, *71*, 2267–2271. [[CrossRef](#)]
34. Catalán, J.; Elguero, J. Fluorescence of C₆₀ and C₇₀. *J. Am. Chem. Soc.* **1993**, *115*, 9249–9252. [[CrossRef](#)]
35. Ma, B.; Sun, Y.P. Fluorescence spectra and quantum yields of [60]fullerene and [70]fullerene under different solvent conditions. A quantitative examination using a near-infrared-sensitive emission spectrometer. *J. Chem. Soc. Perkin Trans.* **1996**, *2*, 2157–2162.
36. Kim, D.; Lee, M. Observation of fluorescence emission from solutions of C₆₀ and C₇₀ and measurement of their excited-state lifetimes. *J. Am. Chem. Soc.* **1992**, *114*, 4429–4430. [[CrossRef](#)]
37. Rani, K.; Sengupta, S. Metal-free FRET macrocycles of perylenediimide and aza-BODIPY for multifunctional sensing. *Chem. Commun.* **2023**, *59*, 1042–1045. [[CrossRef](#)]
38. Mayländer, M.; Nolden, O.; Franz, M.; Chen, S.; Bancroft, L.; Qiu, Y.; Wasielewski, M.R.; Gilch, P.; Richert, S. Accessing the triplet state of perylenediimide by radical-enhanced intersystem crossing. *Chem. Sci.* **2022**, *13*, 6732–6743. [[CrossRef](#)] [[PubMed](#)]
39. Wang, X.-F.; Zhang, X.-R.; Wu, Y.-S.; Zhang, J.-P.; Ai, X.-C.; Wang, Y.; Sun, M.-T. Two-photon photophysical properties of tri-9-anthrylborane. *Chem. Phys. Lett.* **2007**, *436*, 280–286. [[CrossRef](#)]
40. Bisht, H.; Singh, A.P.; Jit, S.; Mishra, H. Effect of concentration on the photophysics of solution of [6,6]-phenyl C₆₁ butyric acid methyl ester (PCBM) in chloroform. *J. Lumin.* **2023**, *258*, 119808. [[CrossRef](#)]

Disclaimer/Publisher's Note: The statements, opinions and data contained in all publications are solely those of the individual author(s) and contributor(s) and not of MDPI and/or the editor(s). MDPI and/or the editor(s) disclaim responsibility for any injury to people or property resulting from any ideas, methods, instructions or products referred to in the content.